Hydrol. Earth Syst. Sci., 21, 5459–5476, 2017
https://doi.org/10.5194/hess-21-5459-2017

Hydrology and Earth System Sciences
Open Access
EGU

Impact of multiple radar reflectivity data assimilation on the numerical simulation of a flash flood event during the HyMeX campaign

Ida Maiello[1,2], Sabrina Gentile[3,1], Rossella Ferretti[2], Luca Baldini[4], Nicoletta Roberto[4], Errico Picciotti[2,5], Pier Paolo Alberoni[6], and Frank Silvio Marzano[1,2]

[1]Department of Information Engineering, Electronics and Telecommunications, Sapienza University of Rome, Rome, Italy
[2]CETEMPS, Department of Physical and Chemical Sciences, University of L'Aquila, L'Aquila, Italy
[3]Institute of Methodologies for Environmental Analysis, CNR IMAA, Potenza, Italy
[4]Institute of Atmospheric Sciences and Climate, CNR ISAC, Rome, Italy
[5]Himet s.r.l., L'Aquila, Italy
[6]Arpae Emilia Romagna, Servizio Idro-Meteo-Clima, Bologna, Italy

Correspondence to: Ida Maiello (ida.maiello@aquila.infn.it)

Received: 23 June 2016 – Discussion started: 15 July 2016
Revised: 19 August 2017 – Accepted: 26 September 2017 – Published: 7 November 2017

Abstract. An analysis to evaluate the impact of multiple radar reflectivity data with a three-dimensional variational (3-D-Var) assimilation system on a heavy precipitation event is presented. The main goal is to build a regionally tuned numerical prediction model and a decision-support system for environmental civil protection services and demonstrate it in the central Italian regions, distinguishing which type of observations, conventional and not (or a combination of them), is more effective in improving the accuracy of the forecasted rainfall. In that respect, during the first special observation period (SOP1) of HyMeX (Hydrological cycle in the Mediterranean Experiment) campaign several intensive observing periods (IOPs) were launched and nine of which occurred in Italy. Among them, IOP4 is chosen for this study because of its low predictability regarding the exact location and amount of precipitation. This event hit central Italy on 14 September 2012 producing heavy precipitation and causing several cases of damage to buildings, infrastructure, and roads. Reflectivity data taken from three C-band Doppler radars running operationally during the event are assimilated using the 3-D-Var technique to improve high-resolution initial conditions. In order to evaluate the impact of the assimilation procedure at different horizontal resolutions and to assess the impact of assimilating reflectivity data from multiple radars, several experiments using the Weather Research and Forecasting (WRF) model are performed. Finally, traditional verification scores such as accuracy, equitable threat score, false alarm ratio, and frequency bias – interpreted by analysing their uncertainty through bootstrap confidence intervals (CIs) – are used to objectively compare the experiments, using rain gauge data as a benchmark.

1 Introduction

In the last few years, a large number of floods caused by different meteorological events have occurred in Italy. These events mainly affected small areas (few hundreds of square kilometres) making their forecast very difficult. Indeed, one of the most important factors in producing a flash flood was found to be the persistence of the meteorological system over the same area in the presence of specific hydrological conditions (the size and the topography of the drainage basin, the amount of urban use within the basin, and so on), allowing for the accumulation of a large amount of rain (Doswell et al., 1996). In complex orography areas, such the Italian regions, this is largely due to the barrier effect produced by the mountains, such as the Apennines. Moreover, the Mediterranean Basin is affected by a complex meteorology, due to

Impact of Multiple Doppler Radar data assimilation on the numerical simulation of a Flash Flood Event during the HyMeX campaign

I. Maiello[1], S. Gentile[1], R. Ferretti[1,2], L. Baldini[3], N. Roberto [3], E. Picciotti[4,1], P.P. Alberoni[5], F. S. Marzano[6,1]

[1]Centre of Excellence CETEMPS, Department of Physics and Chemistry - University of L'Aquila, L'Aquila, Italy

[2]Danish Meteorological Institute, Copenaghen, Denmark

[3]Institute of Atmospheric Sciences and Climate, CNR ISAC, Roma, Italy

[4]Himet s.r.l, L'Aquila, Italy

[5]Arpa Emilia Romagna - Servizio Idro-Meteo-Clima, Bologna, Italy

[6]Department of Electronic Engineering, Sapienza University of Rome, Rome, Italy

Correspondence to: Ida Maiello (ida.maiello@aquila.infn.it)

Abstract. An analysis to evaluate the impact of assimilating multiple radar data with a three dimensional variational (3D-Var) system on a heavy precipitation event is presented. The main goal is to establish a general methodology to quantitatively assess the performance of flash-flood numerical weather prediction at mesoscale. In this respect, during the first Special Observation Period (SOP1) of HyMeX (Hydrological cycle in the Mediterranean Experiment) campaign several Intensive Observing Periods (IOPs) were launched and nine occurred in Italy. Among them IOP4 is chosen for this study because of its low predictability. This event hit central Italy on 14 September 2012 producing heavy precipitation and causing several damages. Data taken from three C-band radars running operationally during the event are assimilated to improve high resolution initial conditions. In order to evaluate the impact of the assimilation procedure at different horizontal resolution and to assess the impact of assimilating multiple radars data, several experiments using Weather Research and Forecasting (WRF) model are performed. Finally, the statistical indexes as accuracy, equitable threat score, false alarm ratio and frequency bias are used to objectively compare the experiments, using rain gauges data as benchmark.

Keywords: *radar data assimilation, WRF, 3D-Var, HyMeX*

1 Introduction

The scientific community widely recognized the need for high resolution numerical weather prediction (NWP) models to improve the very short term forecast of severe weather events and flash floods. The combination of NWP and weather radar observations has shown improved skill with respect to extrapolation-based techniques (Sun et al., 2014). However, the reliability of the mesoscale NWP models is largely dependent on the initial and lateral boundary conditions (IC and BC), and at the resolution of kilometers even more critical because of the lack of high resolution observations, beside for radar data. Several studies in the meteorological area have shown that the assimilation of appropriate observations into the NWP models, especially radar (Sugimoto et al., 2009) and satellite data (Sokol 2009),

significantly reduces the "spin-up" effect (Daley 1991) and improves the IC and BC of the mesoscale models. Classical observations such as SYNOP (surface synoptic observations) or TEMP (upper level temperature, humidity, and winds observations) have not enough density to describe for example local convection, while radar measurements can provide a sufficient density of data. Maiello et al. (2014) showed the positive impact of the radar data assimilation into the precipitation forecast of a heavy precipitation event in Central Italy. The authors showed the gain by using assimilating radar data with respect to the conventional ones. Similar results are obtained for a case of severe convective storm in Croatia by Stanesic and Brewster (2015).

Weather radar plays a key role in revealing tridimensional structures of convective storms and the related mesoscale and microscale systems (Nakatani, 2015). Xiao and Sun (2007) showed that assimilating radar data into the NWP models at high resolution (2km), the convective systems could be better represented in the model initial conditions. Recent investigations from the meteorological perspective have shown that the assimilation of real-time observations, especially the radar measurements (reflectivity or/and Doppler velocity), into the mesoscale NWP models can improve the rainfall forecast for the next few hours (e.g. Xiao et al., 2005; Sokol and Rezacova, 2006; Stephan et al., 2008; Dixon et al., 2009; Salonen et al., 2010).

This study aims at investigating the potential of improving the NWP rainfall forecasts by assimilating multiple radars data. This may have a direct benefit also for hydrological applications, particularly for real time flood forecasting. The novelty of this paper is in exploring impact on the high resolution forecast of the assimilation of multiple radars data in complex orography area such the Italian region to predict intense precipitation. This aim is reached by using the IOP4 of the SOP1 of the HyMeX campaign. The SOP1 was held from 5 September to 5 November 2012; the IOP4 was issued for the Central Italy (CI) target area on 14 September 2012 and it was tagged both as a Heavy Precipitation Event (HPE) and a Flash Flood Event (FFE). Radar reflectivity from three C-band Doppler weather radars is assimilated together with traditional meteorological observations (SYNOP and TEMP) using 3D-Var to improve the Weather Research and Forecasting (WRF) model performance.

The paper is organized as follows. Section 2 provides information on the case study and all the observations to be assimilated by WRF 3D-Var. Section 3 introduces the configuration of the WRF model and the functions of the WRF 3D-Var data assimilation system. The results are presented and evaluated in Section 4. Finally, summary and concluding remarks are given in Section 5.

2 Study area and data

The HyMeX project (http://www.hymex.org) aims at a better understanding of the water cycle in the Mediterranean with emphasis on extreme weather events. The observation strategy of HyMeX is organized in a long-term (4 years) Enhanced Observation Periods (EOP) and short-term (2 months) Special Observation Periods (SOP). During the SOP1, that was held from 5 September to 5 November 2012, three Italian hydro-meteorological site were identified within the Western Mediterranean Target Area (TA): Liguria–Tuscany (LT), northeastern Italy (NEI) and central Italy (CI).

2.1 Case study

During IOP4 a deep trough entered the Tyrrhenian Sea slowly moving south eastward. Advection of cold air along the central Adriatic coast occurred producing instability over central and southern Italy, and enhanced the Bora flow over the northern Adriatic Sea. The heavy precipitations occurred in the morning of September 14 mainly along the central

eastern Italian coast (Marche and Abruzzo regions), associated with the cut-off low over the Tyrrhenian Sea (Figure 1a, c). This structure lasted until 15th September (Figure 1b, d).

Figure 2 shows the interpolated map of 24h accumulated rainfall recorded from rain gauges network from September 14th to September 15th (00:00-00:00UTC) with a maximum accumulated rainfall on the highest peak of Abruzzo region approximately reaching 300 mm in 24hours. DEWETRA is an operational platform used by the Italian Civil Protection Department (DPC) and designed by CIMA Research Foundation to support operational activities at national or international scale. Rain gauges time series of some selected stations in Marche and Abruzzo regions where most of rainfall is accumulated during the event are presented in Figure 3: Fermo and Pintura di Bolognola (Marche region) respectively with nearly 130 mm/24h (Figure 3a) and 180 mm/24h (Figure 3b), Campo Imperatore, Atri and Pescara Colli (Abruzzo region) with respectively nearly 300mm/24h (Figure 3c), 160 mm/24h (Figure 3d) and140 mm/24h (Figure 3e). It is clearly shown (Figure 3) that the incremental accumulation started around 02:00UTC of 14th September: in Fermo, Atri and Pescara Colli most of rainfall was concentrated in the first half of the day, whereas in Pintura di Bolognola and Campo Imperatore, precipitation fell all day long.

It is worthwhile to point out the large amount of hourly precipitation for Pescara and Atri respectively at 05:00UTC and 06:00UTC (red ovals in Fig. 3e and 3d respectively) reaching 45mm/h, indicating convective precipitation, whereas the precipitation on the Gran Sasso (Fig. 3c) was much weaker but lasting longer which allowed for reaching an accumulated amount of 300mm/24h.

Figure 4 reports a graphical tool that combines the Vertical Maximum Intensity (VMI) reflectivity from the Italian radar network (Vulpiani et al., 2008a) together with the Meteosat Second Generation (MSG) 10.8 μm image (in normalized inverted greyscale). VMI values above 45 dBZ are associated with intense precipitation occurred during convective events. Zoom over CI target area shows a line of convective cells along the Apennines in Central Italy due to western flow approaching the orographic barrier.

2.2 Observations to be assimilated

Conventional observations SYNOP and TEMP were retrieved from the ECMWF Meteorological Archival and Retrieval System (MARS). A total of 989 observations (967 SYNOP and 22 TEMP) are ingested into the coarse resolution domain, whereas a total of 338 (331 SYNOP and 7 TEMP) observations are ingested into the high resolution one.
Volumetric reflectivity taken from three C-band Doppler radars operational during the IOP4 have been assimilated to improve IC. Radars have different technical characteristics and were operated with different scanning strategies and operational settings. Data from the single polarization Doppler Mt. Midia radar (MM, 42°03’28’’ N, 13°10’38’’E, h=1760m ASL, n°elevations=4, temporal resolution=15 min, range resolution=500 m) are provided by the Centro Funzionale of Abruzzo Region. The data from the dual polarization Doppler Polar 55C radar (POL, 41° 50’ 24” N, 12° 38’ 50”E, h=102 m ASL, n°elevations=6 or 8, temporal resolution=5 min, range resolution=75 m) are provided by ISAC-CNR of Rome; finally, data from the dual polarization Doppler San Pietro Capofiume radar (SPC, 44°23’24”N, 11°22’12”E, h=31m ASL, n°elevations=6, temporal resolution=15 min, range resolution=250 m) are provided by Arpa Emilia Romagna. MM and SPC radars are included in the Italian radar network, while Polar 55C is a research radar working on demand which was operational during HyMeX IOPs (Roberto et al., 2016).

It is well known that radar observations can be affected by several sources of errors, mainly due to ground clutter, attenuation due to propagation or beam blocking, anomalous propagation and radio interferences. For this reason, a preliminary procedure to correct acquired radar reflectivity from the three radars is applied before the assimilation procedure consisting of the following 2 steps:

- pre-processing consists of a first quality check of radar volumes where radar pixel affected by ground clutter and anomalous propagation were filtered. Furthermore, Z was corrected for attenuation using a methodology based on the specific differential phase shift (K_{dp}) available for dual polarization radars (Vulpiani et al, 2015);
- conversion to the model format is applied to all radars data.

3 Methodology and sensitivity analysis design

The numerical weather prediction experiments are performed in this work using the Advanced Research WRF model Version 3.4.1. WRF is a non-hydrostatic, primitive-equation, mesoscale meteorological model with advanced dynamics, physics and numerical schemes, where the sigma coordinates are adopted to describe the vertical levels. Detailed descriptions of the model can be found in Skamarock et al. (2008) and also on the WRF user website (http://www2.mmm.ucar.edu/wrf/users/). WRF set up, advanced implementation and numerical investigations for flash flood forecast are described in this section

3.1 WRF model set up

In this study, a configuration using two domains run independently is used: a 12km domain (263x185) that covers central Europe and west Mediterranean basin (referred as D01) is initialized using the European Centre for Medium-Range Weather Forecasts (ECMWF) analyses at 0.25 degrees of horizontal resolution; an innermost domain, that covers the whole Italy (referred as D02), with a grid space of 3 km (445x449) using as BC and IC the output of the previous forecast at 12km. Both domains run with 37 unequally spaced vertical levels, from the surface up to 100 hPa (Figure 5).

The WRF model has options for different physical parameterizations such as the boundary layer, the convection and radiation schemes, etc. The performance of a mesoscale model is highly dependent on the parameterization schemes, especially convection, which might be suitable for one ‘storm type’ but inappropriate for another. The main physics packages used in these experiments are set as for the operational configuration used at CETEMPS (Ferretti et al., 2014), which include (Skamarock et al., 2008): the “New” Thompson et al. 2004 microphysics scheme, the Mellor-Yamada-Janjic scheme for the planetary boundary layer, the Goddard shortwave radiation scheme and the rapid radiative transfer model longwave radiation scheme, the Eta similarity scheme for the description of the surface layer and the Noah Land Surface Model to present the land surface physics. A few preliminary tests are performed to assess the best cumulus parameterization scheme to be used both for the coarse and finest resolution domain for this event. Hence the following parameterizations are tested: the new Kain–Fritsch, and the Grell 3D scheme, which is an improved version of the Grell-Deveneyi scheme that may also be used on high resolution (only on coarser domain in our simulations) if subsidence spreading (option cugd_avedx) is turned on. Based on the results of these two cumulus parameterization schemes, the one producing the best precipitation forecast will be used to investigate the impact of the data assimilation.

3.2 3D-Var data assimilation system

Data assimilation is the technique by which observations are combined with a NWP product (called the *first guess* or *background forecast*) and their respective error statistics to provide an improved estimate (named the *analysis*) of the atmospheric (or oceanic) state (Skamarock et al., 2008). The variational data assimilation technique achieves this through the iterative minimization of a prescribed cost function (or penalty) (Ide et al., 1997):

$$J(\boldsymbol{x}) = J^b(\boldsymbol{x}) + J^0(\boldsymbol{x}) = \frac{1}{2}\{[\boldsymbol{y}^0 - H(\boldsymbol{x})]^T \boldsymbol{R}^{-1}[\boldsymbol{y}^0 - H(\boldsymbol{x})] + (\boldsymbol{x} - \boldsymbol{x}^b)^T \boldsymbol{B}^{-1}(\boldsymbol{x} - \boldsymbol{x}^b)\}, \quad (1)$$

where $\boldsymbol{x}$ is the unknown analysis state vector, found by minimizing the cost function $J(\boldsymbol{x})$, $\boldsymbol{x}^b$ is the first guess state vector of the NWP model, $\boldsymbol{y}^0$ is the assimilated observation vector and $\boldsymbol{y}=H(\boldsymbol{x})$ is the forward model derived observation transformed from the analysis $\boldsymbol{x}$ by the observation operator H for comparison against $\boldsymbol{y}^0$.

The minimization of the cost function $J(\boldsymbol{x})$, shown by Equation (1), represents a posteriori maximum likelihood (minimum variance) estimate of the true atmosphere state, given the two sources of a priori data: the first guess $\boldsymbol{x}^b$ and the observation vector $\boldsymbol{y}^0$ (Lorenc, 1986). The fit to individual observation points is weighted by the estimates of their errors, i.e. $\boldsymbol{B}$ and $\boldsymbol{R}$, which are the background covariance error matrix and the observation covariance error matrix, respectively.

The 3D-Var system developed by Barker et al. (2003, 2004) is used in this study in tandem with the WRF model for assimilating radar reflectivity and the conventional observations SYNOP and TEMP. Its configuration is based on an incremental formulation of the variational problem, producing a multivariate incremental analysis for pressure, wind, temperature and relative humidity in the model space. The incremental cost function minimization is performed in a preconditioned control variable space. The preconditioned control variables are stream function, unbalanced potential velocity, unbalanced temperature, unbalanced surface pressure and pseudo relative humidity. In the case of additional assimilation of the radar reflectivity, the total water mixing ratio q_t is chosen as the moisture control variable instead of pseudo relative humidity. The following Equation (2) shows the observation operator used to calculate the model-derived reflectivity for the comparison with the observed one (Sun and Crook, 1997):

$$Z = 43.1 + 17.5\, log(\rho q_r), \quad (2)$$

where Z is the co-polar radar reflectivity factor in dBZ, ρ is the air density in kg/m^3 and q_r is the rainwater mixing ratio. Since the total water mixing ratio q_t is used as the control variable, the partitioning of the moisture and hydrometeor increments is necessary during the minimization procedure. A warm rain parameterization (Dudhia, 1989) is adopted in WRF 3D-Var, exploiting a constraint based on the relation among rainwater, cloud water, moisture and temperature. When rainwater information, through the reflectivity factor expression in Equation (2), enters the minimization iteration procedure, the forward warm rain process and its backward adjoint distribute the information to the increments of other variables under the constraint of the warm rain parameterization scheme.

The performance of the data assimilation system largely depends on the goodness of the background error covariance (BEC), that is the matrix $\boldsymbol{B}$ in Equation (1). In this study, a domain specific background error statistics is generated based on the forecast data from the same domain. The background errors are applied to the same set of the control variables, stream function, unbalanced potential velocity, unbalanced temperature, unbalanced surface pressure, and

pseudo-relative-humidity. Furthermore, the control variables are in eigenvector space and uses an empirical orthogonal function (EOF) to represent the vertical covariance. The background error covariance matrix is generated via the National Meteorological Center (NMC) method (Parrish and Derber, 1992) for both domains. To estimate the NMC-based error statistics, two forecasts are performed every day for the entire SOP1 period (5 September - 5 November 2012): a 24h forecast (starting from 00:00UTC) and a 12h forecast (starting from 12:00UTC) valid at the same time. The differences between the two forecasts at t+24 and t+12 are used to calculate the domain-averaged error statistics.

3.3 Design of the numerical experiments

The simulations on the coarser resolution domain (D01) are run from 12:00UTC of 13 September 2012 and integrated for the following 96 hours, whereas runs on the finest resolution domain started at 00:00UTC of September 14 for a total of 48 hours of integration. The 00:00UTC coarser resolution WRF forecast is used as the first guess (FG) in the 3D-Var experiment that is the analysis time in the assimilation procedure. After assimilation, the lateral and lower boundary conditions are updated for the high resolution forecast. Finally, the new initial and boundary conditions are used for the model initialization (in a warm start regime) at 00:00UTC. As already pointed out a set of preliminary experiments are performed using different cumulus convective scheme to assess the best one to be used. The following experiments are performed without assimilation and using the convective scheme on the coarser resolution domain only: KAIN-FRITSCH (KF_MYJ); GRELL3D (GRELL3D_MYJ); GRELL3D associated to the CUGD factor (GRELL3D_MYJ_CUGD). A summary of these numerical experiments is given in Table 1.

The analysis of the results of these set of experiments allows establishing the best model configuration for the radar data assimilation experiments. The data assimilation (DA) experiments aim to investigate:

1. the impact of the assimilation at low and high resolution by assimilating both conventional and non-conventional data at both resolutions;
2. the impact of the assimilation of different types of observations;
3. the impact of the different radars, which is investigated by performing experiment by assimilating conventional data and then adding radar one by one.

The following experiments are performed: i) the control simulation (CTL) without data assimilation; the assimilation of conventional data (SYNOP and TEMP) only (CON_LR_12KM); ii) the assimilation of radar data from MM only (CONMM_LR_12KM) are added; iii) the assimilation of POL radar is added to the previous experiments (CONMMPOL_LR_12KM); iv) the assimilation of the third radar data is added to the previous (CONMMPOLSPC_LR_12KM). Finally, an experiment to assess the role of the outer loop is performed (CONMMPOLSPC3OL_LR_12KM). The multiple outer loops strategy (Rizvi et al., 2008) allows for including non-linearity in the observation operators and for assessing the influence of observations entering for each cycle. The non-linear problem is solved iteratively as a sequence of linear problems by running more than one analysis outer loop, so the assimilation system is able to ingest more observations. The experiments are summarized in (Table 2).

The MET (Model Evaluation Tools) application (DTC, 2013), developed at the DTC (Developmental Testbed Center, NCAR), has been used to objectively evaluate the 12 hours accumulated precipitation produced by WRF on the high resolution domain. The observations used for the statistical evaluation were obtained from the Platform DEWETRA of the Department of Civil Protection and the comparison has been performed over the central Italy target area using about 3000 rain gauges with a good cover throughout the area.

4 Results and discussion

In this section the results will be presented and discussed following the rationale of the previously introduced experiments and using statistical indexes for performance quantitative assessment.

4.1 Sensitivity test to cumulus parameterization

The 24h accumulated rainfall on Central Italy simulated by the model both on D01 (left column) and D02 (right column) using a different cumulus parameterization scheme (Fig. 6, on line 1 Kain-Fritsch, on line 2 Grell 3D, on line 3 Grell 3D and cugd_avedx=3 activated) is shown. Comparing the model outputs (Fig. 6) and the rain gauge observations (Fig. 2), it is worth noting that best performance on D01 is obtained by Grell 3D which is able to simulate the peak precipitation cumulated in 24 hour (between 200 and 300 mm) over Gran Sasso (Fig. 6, lines 2 and 3), whereas Kain-Fritsch (Fig. 6a) completely misses the peak of rainfall on Abruzzo region (red spot in Fig. 2). Moreover, the rainfall pattern is not properly reproduced.

Furthermore results suggest that the spreading of the convective downdraft over several grid points allows for improving the rainfall distribution at both resolution: both the main cells of heavy rainfall are correctly separated over Abruzzo both on D01 and D02 (Fig. 6e and 6f) and the rainfall pattern along the northeast coast of Abruzzo region is also reproduced (Fig. 6f). The statistical indices computed using MET are showed in the next figure. The MET statistical analysis support the previous finding: the GRELL3D_MYJ_CUDG (blue curve Fig. 7) in the range 5-30 mm/12h shows higher performances in terms of accuracy (ACC, Fig 7a), equitable threat score (ETS, Fig. 7b) and false alarm ratio (FAR, Fig. c) than the other two simulations. Also the frequency bias (FBIAS, Fig. 7d, green and blue curves) indicates the simulations performed with Grell 3D as the one producing better results. Indeed it shows values closer to 1 (the best value) than Kain-Fritsch (red curve). Finally, the mean error (ME, Fig. 7e, blue curve) for Grell 3D with cugd_avedx activated has values close to 0 (perfect value).

Here after GRELL3D_MYJ_CUDG is referred as the control (CTL) experiment performed without any data assimilation. Therefore, a new set of simulations are performed following the previous strategies: data assimilation on low or high resolution domains or on both domains simultaneously; conventional data and/or radar data assimilation.

4.2 Impact of conventional and radar data assimilation on rainfall forecast: low versus high resolution

In figure 8 a preliminary comparison among the low resolution (12km) simulations is shown. The control simulation (CTL) without data assimilation is shown in Figure 8a; whereas the other panels show the experiments performed using the data assimilation.

Observing the outputs of different experiments (Fig. 8) listed in Table 2, best simulation is found for CONMMPOLSPC_LR_12KM (Fig.8e) for which an attempt to reproduce the rainfall maximum over Campo Imperatore (black arrow) is found: the rainfall amount is very well simulated, however a cell displacement is noticeable. Furthermore a quite good attempt to forecast precipitation along the coasts (black oval) is also found.

The statistical indices (Fig. 9) support this finding: the brown curve (CONMMPOLSPC_LR_12KM) is producing the best ACC and FAR for all thresholds, except for ETS where good values are found only for thresholds lower than 20 mm/12h.

Similarly to the above comparison, high resolution results are presented in figure 10 obtained performing data assimilation only on 12km domain (column 1), only on 3km (column 2) and both on 12km and 3km (column 3); to the top of figure 10 the CTL experiment on D02 is shown. Figure 10 is organized as follows: viewing panels by line on line 1 all the simulations with conventional data assimilation (CON*) only are found; on line 2 all the experiments with the assimilation of the data from Mt. Midia radar added (CONMM*); on line 3 all the experiments with the assimilation of the data from 2 C-band radars added (CONMMPOL*); on line 4 all the experiments with the assimilation of the data from all 3 C-band radars added (CONMMPOLSPC*); on line 5 the simulations where the strategy of outer loop is adopted (CONMMPOLSPC3OL*). For these experiments the values of the main statistical indices (ACC, FBIAS, ETS, FAR) have been summarized over tables reporting only two thresholds of precipitation: 1 mm/12h and 20 mm/12h (light and heavy rain regimes).

To the aim of investigating the impact of the assimilation at different resolutions, we start analyzing figure 10 by column and comparing it with the observation (fig. 2); the statistical analysis is also used:

- column 1 (12KM): CTL produces an overestimation of the rainfall that is not corrected by the assimilation of conventional data, but assimilating the 3 radars and introducing the 3 outer loops (Fig. 10 column 1 line 4) the main cells are better reproduced. MET indices in Table 3 suggest that CTL and CONMMPOLSPC3OL_HR_12km are the simulations with the best response, secondly CONMM_HR_12KM;
- column 2 (3KM): a partial correction of the rainfall overestimation compared to column 1 is observed especially if all the radars are assimilated and the outer loop strategy is applied; the statistical indices in Table 4 show CONMMPOLSPC3OL_3KM as the best experiment among the assimilated ones;
- column 3 (12KM_3KM): rainfall overestimation was partially corrected compared to columns 1 and 2 by all experiments; the MET statistics in Table 5 shows that CTL and CONMMPOLSPC3OL_3KM_12KM are the experiments that return better values.

Summarizing, the previous analysis suggests that the frequency of rainfall overestimation for higher thresholds has been reduced by radar data assimilation performed only on DOM1. Furthermore, improvements come out for heavy rain regimes when radar data assimilation has been performed on the highest resolution domain, whereas the ingestion of conventional observations produces the worst results since a smaller number of them were assimilated into the finest resolution domain than that the coarser one. The assimilation, operated on both 12 km and 3 km, gives better results than the ones on column 1, but a response worse than the others on column 2 is given for higher thresholds.

To the aim of investigating the impact of the assimilation of different data and radars, we can now analyze the experiments showed in figure 10 by line. The results are compared with the observations of Fig. 2. The following considerations are worth discussing:

- line 1 (CON): a strong reduction of the rainfall is found with respect to CTL if conventional data are assimilated, but the rainfall pattern remains unchanged; statistical indices in Table 6 seem do not improve performances of CTL. The indices values suggest a slightly better performance when the conventional observations are assimilated only on the bigger domain;

- line 2 (CONMM): a further reduction in the precipitation overestimation is found as well as some variations in the pattern of the rainfall; statistics in Table 7 shows that Mt. Midia radar data assimilation improves model performance above all for higher thresholds; conventional observations assimilation in tandem with MM gives better results;
- line 3 (CONMMPOL): a quite strong improvement in the rainfall amount is found for all simulations. From the statistics of Table 8 we have found a worsening of the results especially for heavy rain regimes when POL is added (FBIAS and ETS); a better answer is given by the simulation where assimilation is performed on both domains;
- line 4 (CONMMPOLSPC): a clear correction of the rainfall pattern is found; the overestimation produced by the simulation where all the radars are assimilated on the 3km domain has been corrected by the experiment in which the radars are assimilated both on D01 and D02; statistical indices in Table 9 suggest that the addition of SPC radar improves the results, furthermore they are not better than those where only MM is ingested;
- line 5 (CONMMPOLSPC3OL): the outer loop experiments confirms the overestimation reduction by *12KM_3KM; from Table 10 it seems that the introduction of 3OL improves the indices values above all when the 12km domain is considered; CONMMPOLSPC3OL_12KM_3KM can be considered the best simulation.

In summary, simulations results show that it is better to perform the assimilation of conventional observations on the lowest resolution domain. Regarding the assimilation of radar data, POL is the one that gives the worst results due to significant errors in rainfall detection and thus misleading the WRF model forecast. The outer loop strategy could have an important role in the assimilation procedure, but this latter needs a further investigation because a general rainfall underestimation for higher thresholds is found.

5 Conclusions

The purpose of this paper has been to assess the impact of multiple radar data assimilation on a heavy precipitation event occurred during the SOP1of the HyMeX campaign. A sensitivity study at different domain resolution and using different types of data to improve initial conditions has been performed by assimilating into the WRF model radar reflectivity measurements, collected by three C-band Doppler weather radars operational during the event that hit Central Italy on 14 September 2012. The 3D-Var and MET are the WRF tools used to assess this purpose. First of all, WRF model resposnes to different type of cumulus parameterization have been tested to establish the best configuration and to obtain the control simulation. The latter has been compared with observations and other experiments performed using 3D-Var. The set of assimilation experiments have been conducted following two different strategies: (i) data assimilation at low and high resolution or at both resolutions simultaneously; (ii) conventional data against radar data assimilation. Both have been examined to assess the impact on rainfall forecast.

The major findings of this work have been the following:

- Grell 3D parameterization improves the simulations both on D01and D02 and the use of the spreading factor is an added value in properly predict heavy rainfall over inland of Abruzzo and the rainfall pattern along the northeast coast;

- investigating the impact of the assimilation at different resolutions, best results are showed by the experiments where the data assimilation is performed on both domains 12km and 3km;
- the impact of the assimilation using different types of observations shows improvements if all the radars together with conventional data are assimilated; furthermore MM is the one that better impact the model results because of it has been better detected the event;
- the outer loop strategy allows for further improving positive impact of the assimilation of multiple radars. Moreover, a deeper investigation of multiple outer loops strategy is required to assess its impact.

Analyzing the results obtained in this study, it is not possible to assess which is, in general, the best model configuration since this analysis should be performed systematically with a significant number of case studies. However, this is work is providing a general approach that can encourage to investigate more flash-flood cases in order to make the assimilation of multiple radars data suitable for operational use. In order to confirm and consolidate these initial findings, apart from analyzing more case studies, a "pseudo-operational" testing would be also useful.

Acknowledgements

We are grateful to the Gran Sasso National Laboratories for computing resources support, as well as the National Civil Protection Department and CIMA Research Foundation for rain gauges data using for the model validation. National Center for Atmospheric Research is also acknowledge for WRF model and 3D-Var system.

References

Barker, D.M., Huang, W., Guo, Y.-G., and Bourgeois, A.: A Three-Dimensional Variational (3D-Var) Data Assimilation System For Use With MM5. NCAR Tech. Note, NCAR/TN-453+STR, UCAR Communications, Boulder, CO, 68pp, 2003.

Barker, D.M., Huang, W., Guo, Y.-R., Bourgeois, A., and Xiao, Q.: A Three-Dimensional Variational (3D-Var) Data Assimilation System For Use With MM5: Implementation and Initial Results. *Mon. Wea. Rev.*, 132, 897-914, 2004.

Daley, R.: Atmospheric Data Analysis, Cambridge University Press, Cambridge, UK, 1991.

Developmental Testbed Center, 2013: MET: Version 4.1 Model Evaluation Tools Users Guide. Available at http://www.dtcenter.org/met/users/docs/overview.php. 226 pp.

Dixon, M., Li, Z., Lean, H., Roberts, N., and Ballard, S.: Impact of data assimilation on forecasting convection over the United Kingdom using a high-resolution version of the Met Office Unified

Model, Mon. Weather Rev., 137, 1562–1584, 2009.

Dudhia, J.: Numerical study of convection observed during the winter monsoon experiment using a mesoscale two-dimensional model, J. Atmos. Sci., 46, 3077–3107, 1989.

Ferretti, R., E. Pichelli, S. Gentile, I. Maiello, D. Cimini, S. Davolio, M. M. Miglietta, G. Panegrossi, L. Baldini, F. Pasi, F. S. Marzano, A. Zinzi, S.Mariani, M. Casaioli, G. Bartolini, N. Loglisci, A. Montani, C. Marsigli,A.Manzato, A.

375 Pucillo, M. E. Ferrario, V. Colaiuda, and R. Rotunno: Overview of the first HyMeX Special ObservationPeriod over
376 Italy: observations and model results. Hydr. Earth Syst. Sci., 18, 1953-1977,2014, doi:10.5194/hess-18-1953-2014,
377 2014.

378 Ide, K., Courtier, P., Ghil, M., and Lorenc, A. C.: Unified notation for data assimilation: Operational, sequential and
379 variational, J. Meteorol. Soc. Jpn., 75, 181–189, 1997.

380 Li Y., Wang X., and Xue M., 2008: Assimilation of radar radial velocity data with the WRF ensemble-3DVAR hybrid
381 system for the prediction of hurricane Ike, *Mon. Wea Rev*, vol. 140, pp. 3507–3524.

382 Lorenc, A. C.: Analysis methods for numerical weather prediction, Q. J. Roy. Meteorol. Soc., 112, 1177–1194, 1986.

383 Maiello, I., Ferretti, R., Gentile, S., Montopoli, M., Picciotti, E., Marzano, F. S., and Faccani, C.: Impact of radar data
384 assimilation for the simulation of a heavy rainfall case in central Italy using WRF–3DVAR, Atmos. Meas. Tech., 7,
385 2919-2935, doi:10.5194/amt-7-2919-2014, 2014.

386 Nakatani T., Misumi R., Shoji Y., Saito K., Seko H., Seino N., Suzuki S-I.,Shusse Y., Maesaka T., and Sugawara H. ;
387 Tokyo metropolitan area convection study for extreme weather resilient cities. *BAMS,* 96, ES123-ES126, 2015.

388 Parrish, D.F. and Derber, J.C.: The National Meteorological Center's Spectral Statistical-Interpolation Analysis System.
389 *Mon. Wea. Rev.,* 120, 1747-1763, 1992.

390 Rizvi, S., Guo, Y.-R, Shao, H., Demirtas, M., and Huang, X.-Y.: Impact of outer loop for WRF data assimilation system
391 (WRFDA). 9th WRF Users' Workshop, Boulder, Colorado, 23-27 June 2008.

392 Roberto, N., Adirosi, E., Baldini, L., Casella, D., Dietrich, S., Gatlin, P., Panegrossi, G., Petracca, M., Sanò, P., and
393 Tokay, A.: Multi-sensor analysis of convective activity in central Italy during the HyMeX SOP 1.1, Atmos. Meas.
394 Tech., 9, 535-552, doi:10.5194/amt-9-535-2016, 2016.

395 Salonen K, Haase G, Eresmaa R, Hohti H, Järvinen H. 2010. Towards the operational use of Doppler Radar radial
396 winds in HIRLAM. Atmospheric Research 100: 190–200.

397 Skamarock, W.C., Klemp, J.B., Dudhia, J., Gill, D.O., Barker, D.M., Duda, M. G., Huang, X.-Y., Wang, W., and
398 Powers, J. G.: A description of the Advanced Reasearch WRF Version 3. NCAR Technical Note. TN 475+STR, 113
399 pp., available from www.mmm.ucar.edu/wrf/users/docs/arw_v3.pdf (last access: January 2012), 2008.

400 Sokol, Z. and Rezacova, D.: Assimilation of Radar reflectivity into the LMCOSMO model with a high horizontal
401 resolution, Meteorol. Appl., 13, 317–330, 2006.

402 Sokol, Z.: Effects of an assimilation of Radar and satellite data on a very short range forecast of heavy convective
403 rainfalls, Atmos. Res., 93, 188–206, 2009.

404 Stanesic A., and K.A. Brewester: Impact of Radar Data Assimilation on the Numerical Simulation of a Severe Storm in
405 Croatia. Met.Zeit.DOI 10.1127/metz/2015/0574, 2015.

406 Stephan K, Klink S, Schraff C. 2008. Assimilation of Radar derived rain rates into the convective scale model COSMO-
407 DE at DWD. QuarterlyJournal of the Royal Meteorological Society 134: 1315–1326.

408 Sugimoto, S., Crook N.A., Sun J., Xiao Q., and Barker D.M., 2009: An examination of WRF 3D-VarRadar data
409 assimilation on its capability in retrieving unobserved variables and forecasting precipitation through observing system
410 simulation experiments. *Mon. Wea. Rev.*, 137, 4011-4029, DOI:10.1175/2009MWR2839.1.

411 Su, J. Xue, M., Wilson J. W., Zawadzki I., Ballard S.P., Onvlee-Hooimeyer J., Joe P., Barker D.M., Li P-W., Golding
412 B., Xu M., and Pinto J.: Use of NWP for nowcasting convective precipitation, recent progress and challenges. *BAMS,*
413 95, 409-426, 2014.

414 Sun, J. and Crook, N.A.: Dynamical and Microphysical Retrieval from Doppler RADAR Observations Using a Cloud
415 Model and Its Adjoint. Part I: Model Development and Simulated Data Experiments. *J. Atmos. Sci.,* 54, 1642-1661,
416 1997.

417 Thompson, G., R. M. Rasmussen, and K. Manning, 2004: Explicit forecasts of winter precipitation using an improved
418 bulk microphysics scheme. Part I: Description and sensitivity analysis.

419 Mon. Wea. Rev.,132, 519–542.

420 Vulpiani G., Pagliara, P., Negri, M., Rossi, L., Gioia, A., Giordano, P., Alberoni, P. P., Cremonini, R., Ferraris, L., and
421 Marzano, F. S.: The Italian radar network within the national early-warning system for multi-risks management, Proc.
422 of Fifth European Conference on Radar in Meteorology and Hydrology (ERAD 2008), 184, Finnish Meteorological
423 Institute, Helsinki, 30 June-4 July, 2008a.

424 Vulpiani, G., Baldini, L., and Roberto, N.: Characterization of Mediterranean hail-bearing storms using an operational
425 polarimetric X-band radar, Atmos. Meas. Tech., 8, 4681-4698, doi:10.5194/amt-8-4681-2015, 2015.

426 Wang X., Barker D. M., Snyder C., and Hamill T. M., 2008: "A hybrid ETKF-3DVAR data assimilation scheme for the
427 WRF model. Part I: observation system simulation experiment," Monthly Weather Review, vol. 136, no. 12, pp. 5116–
428 5131.

429 Xiao, Q., Kuo, Y.-H., Sun, J. and Lee, W.-C.: Assimilation of Doppler RADAR Observations with a Regional 3D-Var
430 System: Impact of Doppler Velocities on Forecasts of a Heavy Rainfall Case. *J. Appl. Meteor.,*44, 768-788, 2005.

431 Xiao, Q. and Sun, J.: Multiple-RADAR Data Assimilation and Short-Range Quantitative Precipitation Forecasting of a
432 Squall Line Observed during IHOP_2002. *Mon. Wea. Rev.*, 135, 3381-3404, 2007.

433

434

435

436

437

438

439

440

441

442

443

444 **LIST OF FIGURES**

445

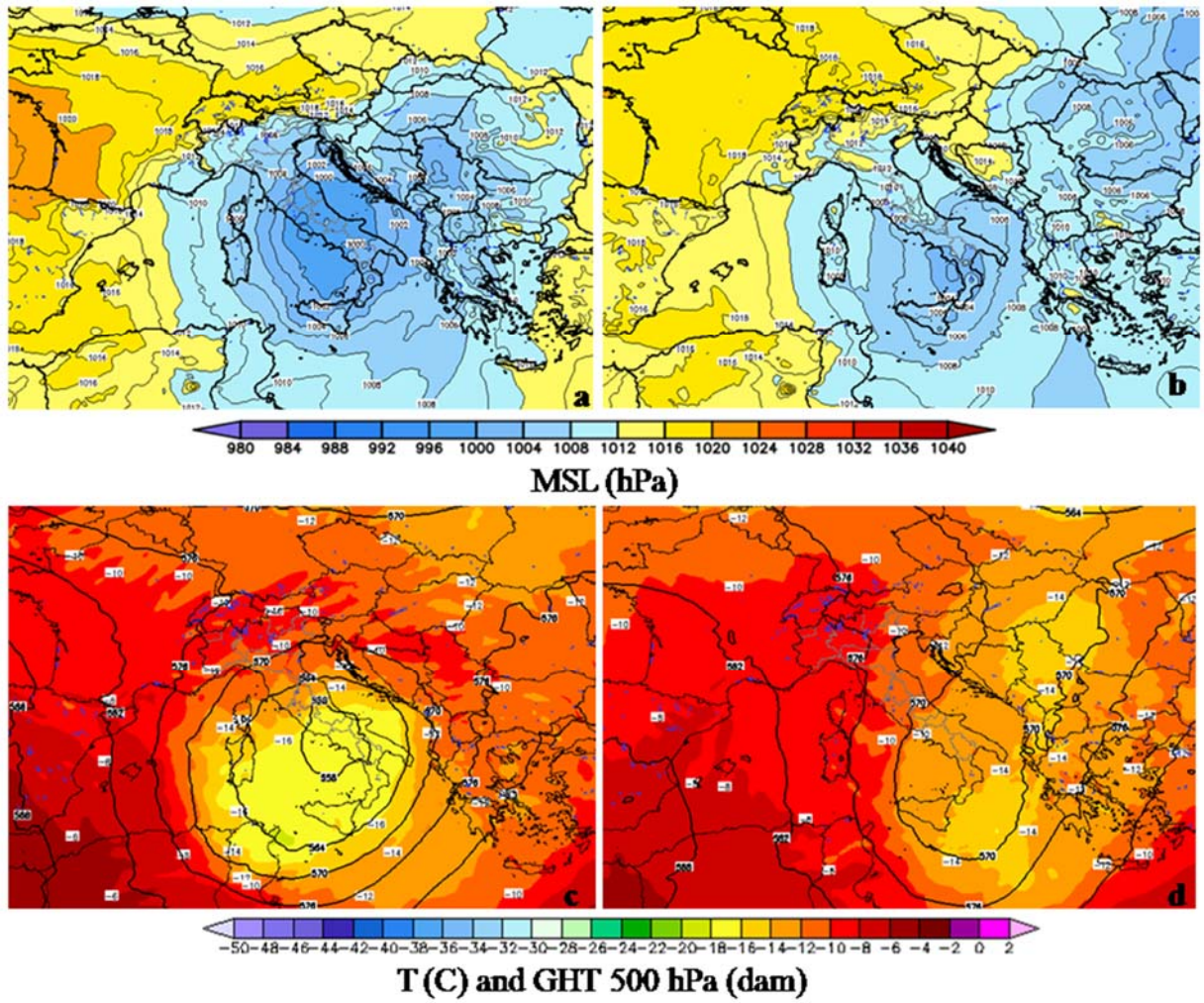

446

447 **Figure 1: Mean sea level pressure (a, b), temperature and geopotential height at 500 hPa (c, d) at 12:00UTC on 14 September**
448 **and 15 September 2012, respectively.**
449

450

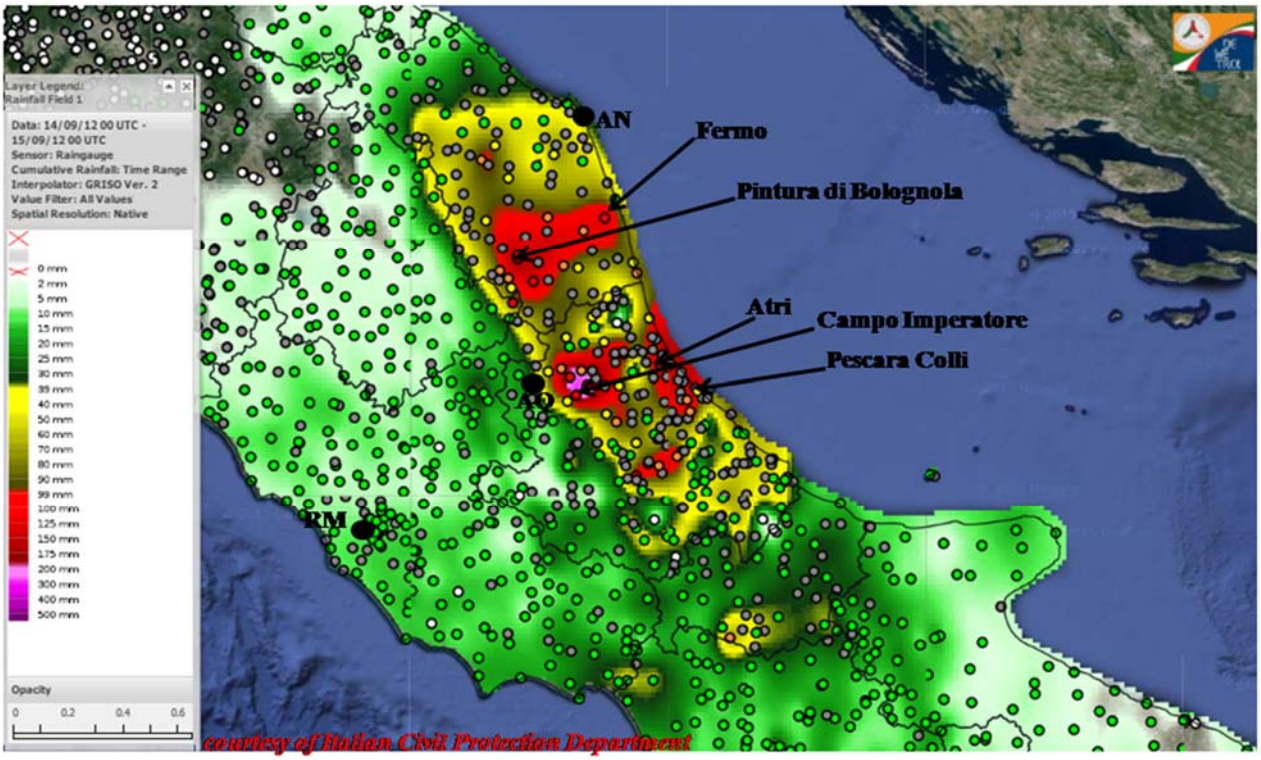

Figure 2: Interpolated map of 24h accumulated rainfall from 00:00UTC of 14 September 2012 over Abruzzo and Marche regions from DEWETRA system obtained by rain gauges measurements. Black contours are the administrative boundaries of Regions.

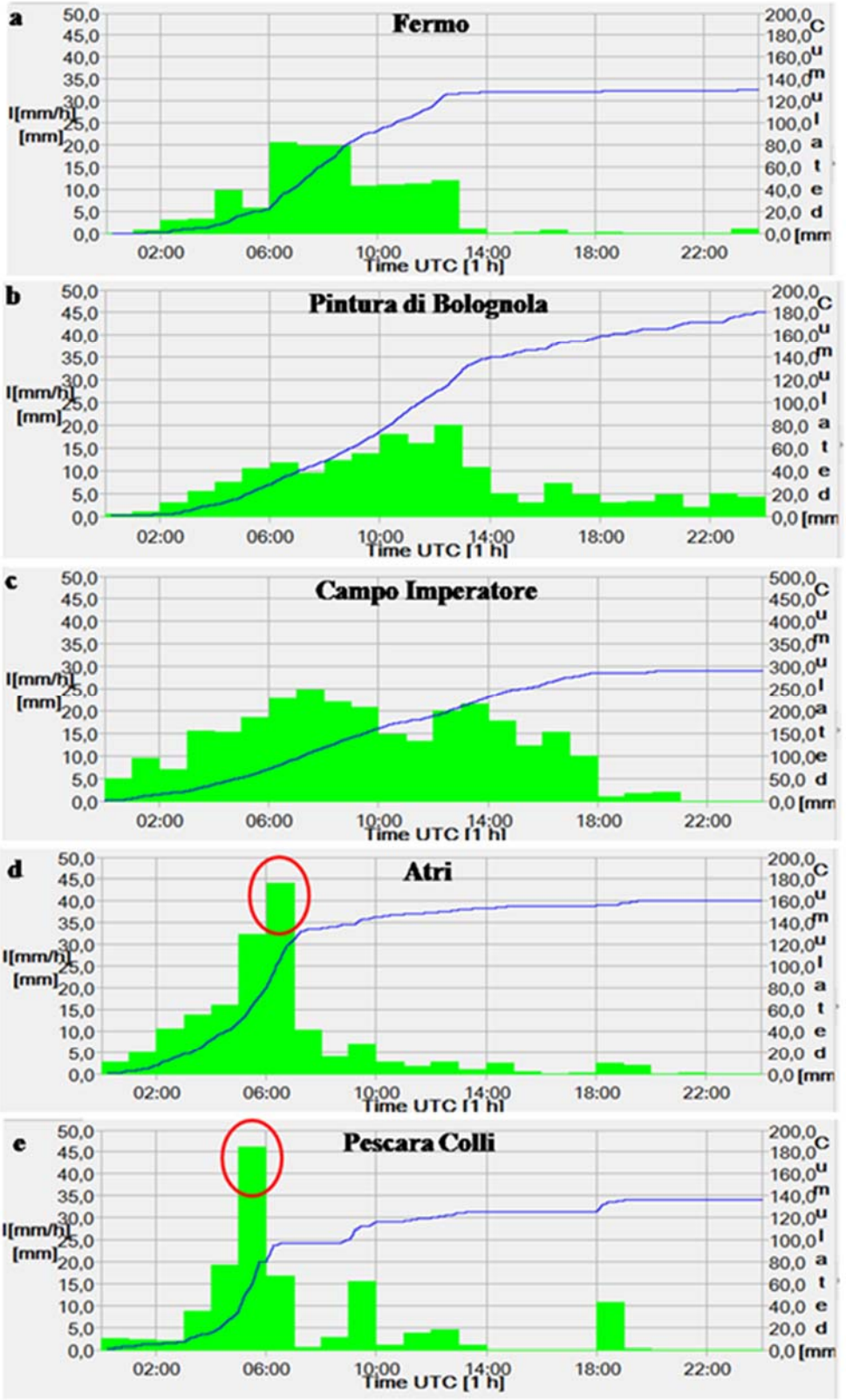

Figure 3: Rain gauges time series of some selected stations in Marche (a and b) and Abruzzo (c, d and e) regions during the event on 14 September 2012. The green histogram represents the hourly accumulated precipitation (scale on the left); the blue line represents incremental accumulation within the 24h (scale on the right). (*courtesy of Italian Civil Protection Department*)

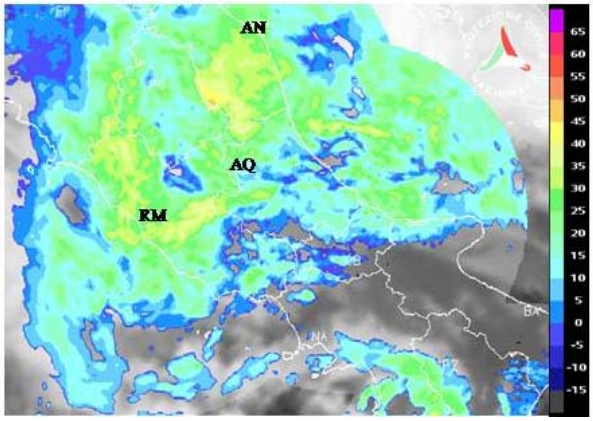

Figure 4: Zoom over CI of the VMI on 14 September 2012 at 08:00UTC from the Italian radar network overlapped with the MSG (IR 10.8) at 07:30UTC. (*courtesy of Italian DPC*)

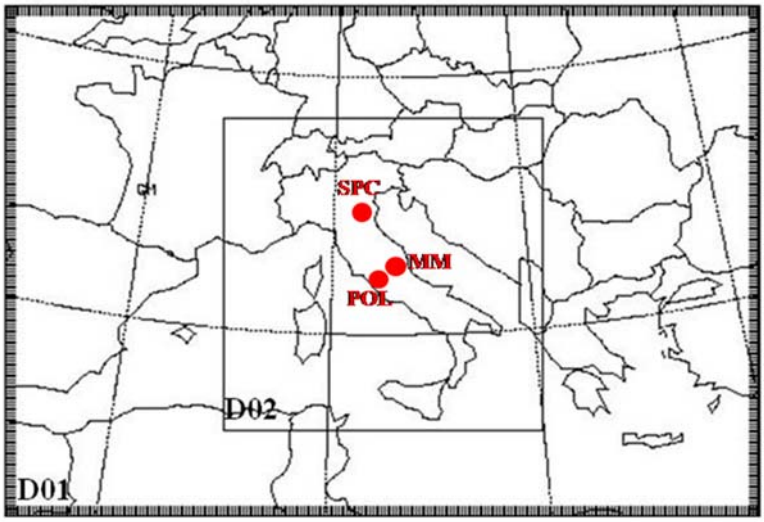

Figure 5: WRF nest-down domains configuration: the two domains have respectively resolution of 12 and 3 km. The high resolution D02 over Italy includes Mt. Midia (MM), ISAC-CNR (POL) and San Pietro Capofiume (SPC) radars (red dots in the figure).

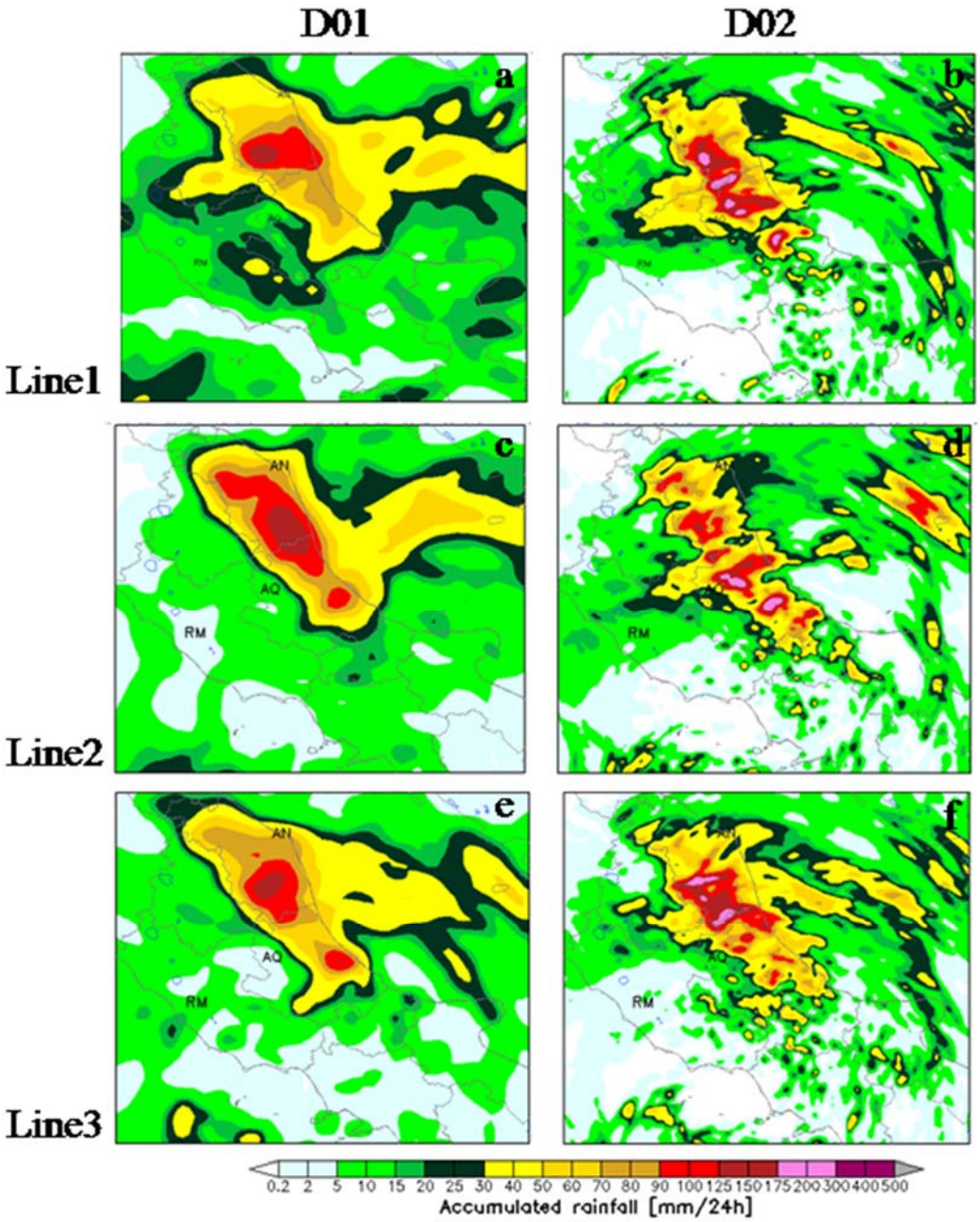

471

472 **Figure 6: WRF accumulated 24h rainfall forecast on Central Italy from 00:00UTC of 14 September 2012: a,b) D01 and D02**
473 **respectively run with Kain-Fritsch; c,d) D01 and D02 respectively run with Grell 3D; e,f) D01 and D02 respectively run with**
474 **Grell 3D and cugd_avedx=3 activated.**

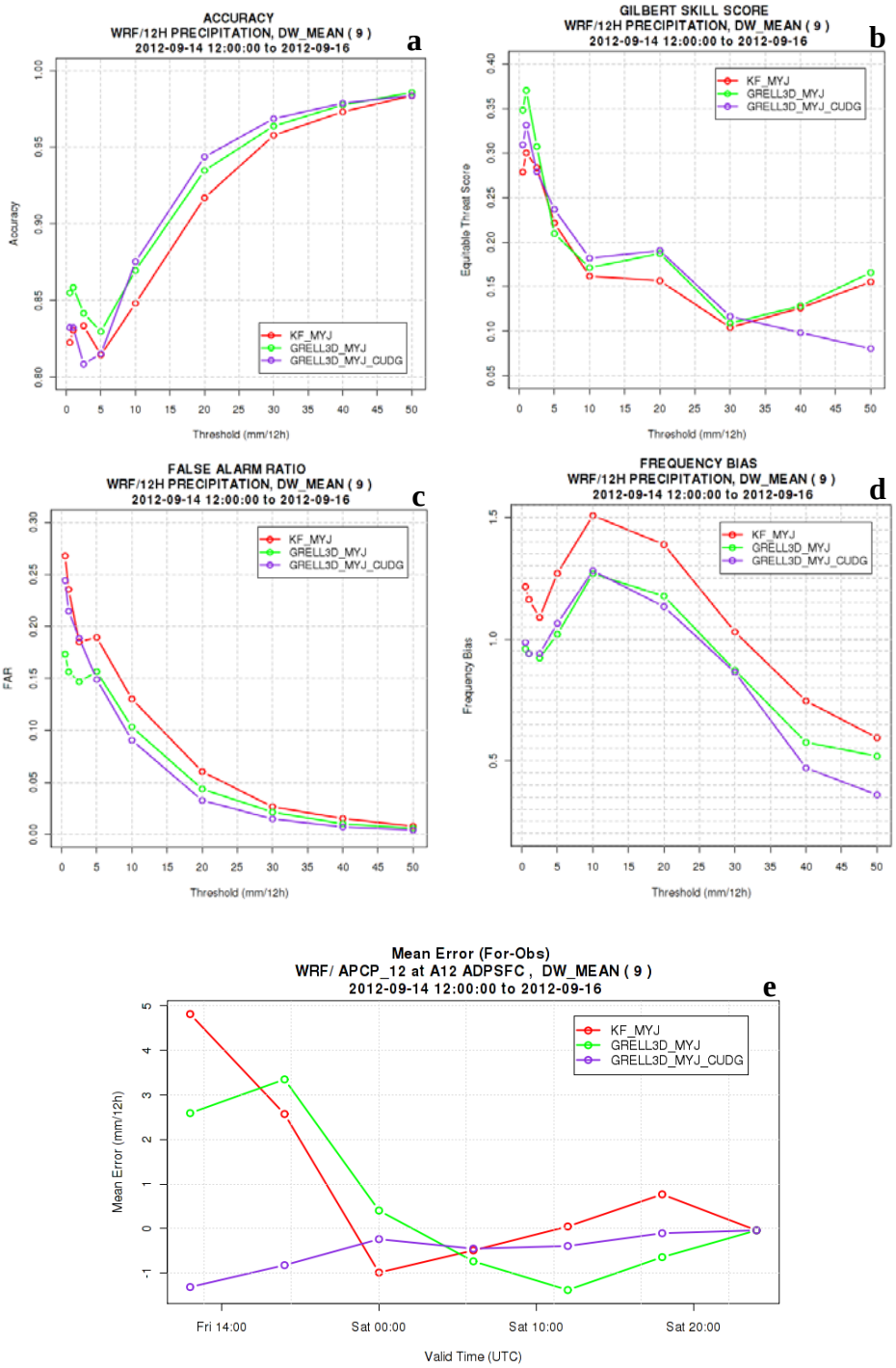

Figure 7: Forecast Accuracy (a), Equitable Threat Score (b), False Alarm Ratio (c), Frequency Bias (d) as a function of threshold and Mean Error (e) as a function of time. The red and green curves indicate Kain-Fritsch and Grell 3D simulations respectively, whereas the blue curve represents Grell 3D experiment with cugd_avedx=3 activated.

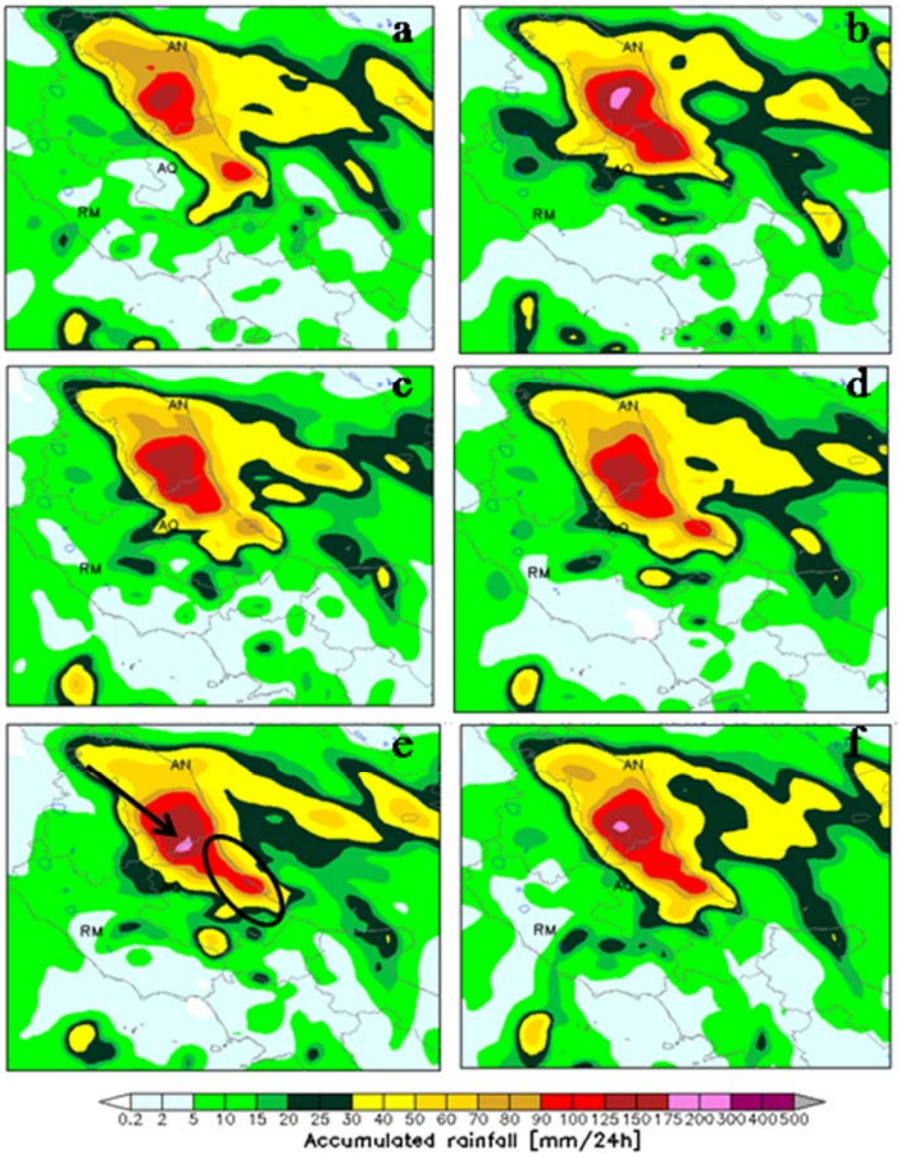

Figure 8: WRF D01 accumulated 24h rainfall forecast on Central Italy from 00:00UTC of 14 September 2012: a) WRF D01 CTL; b)WRF D01 CON_LR_12KM;c) WRF D01CONMM_LR_12KM;d)WRF D01CONMMPOL_LR_12KM;e) WRF D01CONMMPOLSPC_LR_12KM; f) WRF D01CONMMPOLSPC3OL_LR_12KM.

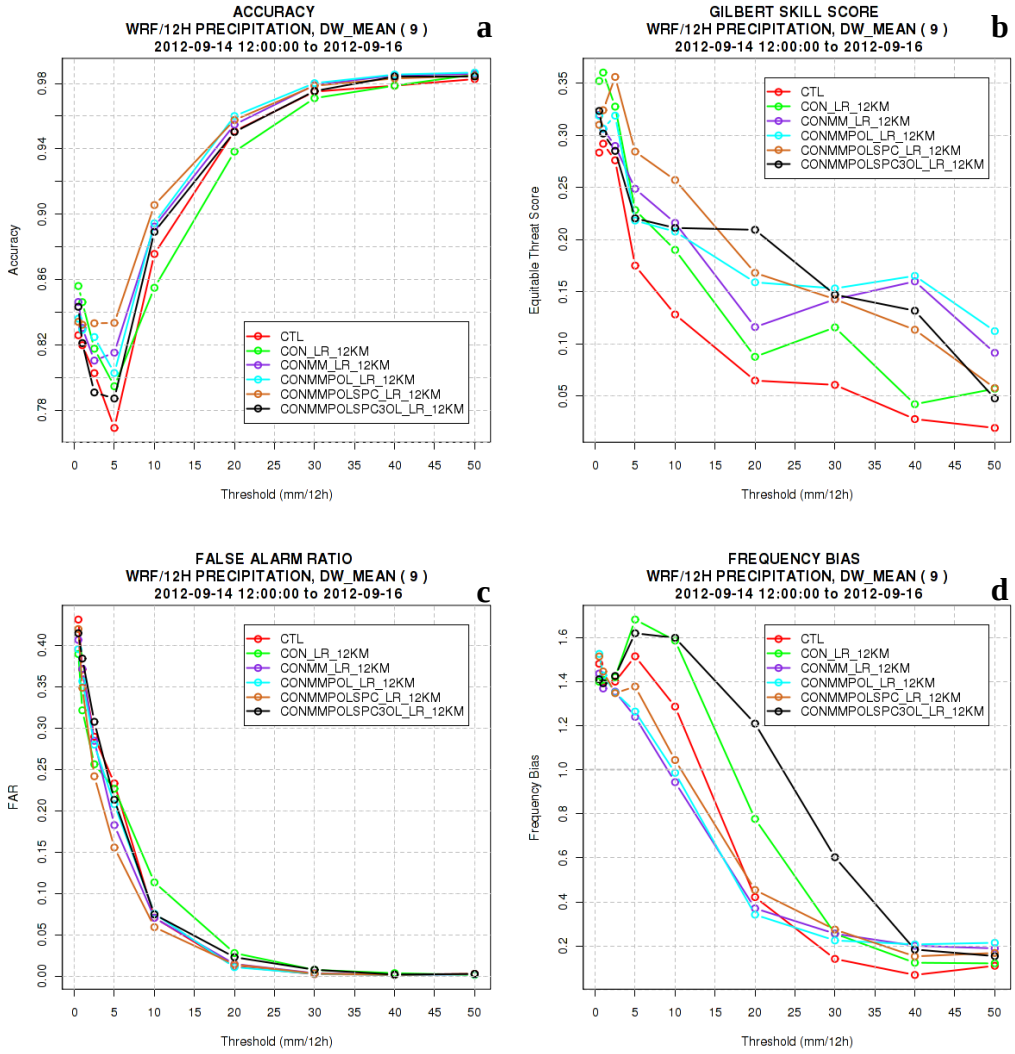

Figure 9: Forecast Accuracy (a), Equitable Threat Score (b), False Alarm Ratio (c) and Frequency Bias (d) as a function of threshold. The red curve indicates CTL experiment, the green curve CON_LR_12KM, the blue curve CONMM_LR_12KM, the cyan curve CONMMPOL_LR_12KM, the brown curve CONMMPOLSPC_LR_12KM, the black curve CONMMPOLSPC3OL_LR_12KM.

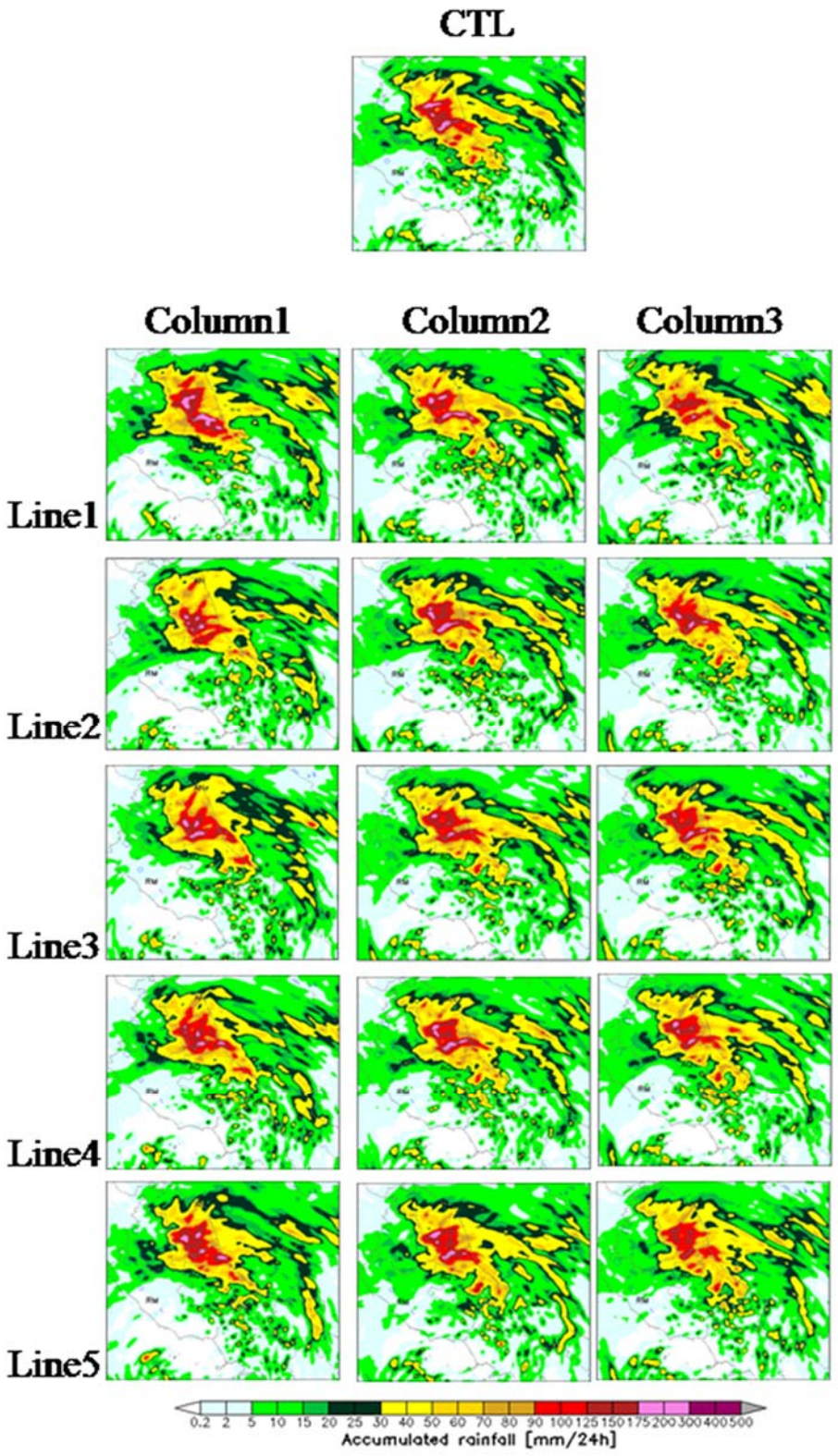

493

494 **Figure 10: WRF D02 accumulated 24h rainfall forecast on Central Italy from 00:00UTC of 14 September 2012: CTL**
495 **simulation (top center); on each column simulations obtained performing data assimilation at different resolutions (*12KM,**
496 ***3KM, *12KM_3KM); on each line simulations performed assimilating different kinds of data (CON*, CONMM*,**
497 **CONMMPOL*,CONMMPOLSPC*, CONMMPOLSPC3OL*).**

498

499

500 **Table 1: List of experiments to assess the cumulus parameterization.**

Experiment	Cumulus	Grid Resolution	Assimilation Synop+Temp	Assimilation Radar
KF_MYJ	KAIN-FRITSCH	12KM/3KM	NO	NO
GRELL3D_MYJ	GRELL3D	12KM/3KM	NO	NO
GRELL3D_MYJ_CUGD (CTL)	GRELL3D+CUGD	12KM/3KM	NO	NO

501

502 **Table 2: List of experiments to test the impact of data assimilation.**

Experiment	Cumulus	Grid Resolution	Assimilation Synop+Temp	Assimilation Radar
CTL	GRELL3D+CUGD	12KM/3KM	NO	NO
CON	GRELL3D+CUGD	12KM/3KM/BOTH	YES	NO
CONMM	GRELL3D+CUGD	12KM/3KM/BOTH	YES	MM
CONMMPOL	GRELL3D+CUGD	12KM/3KM/BOTH	YES	MM+POL
CONMMPOLSPC	GRELL3D+CUGD	12KM/3KM/BOTH	YES	MM+POL+SPC
CONMMPOLSPC3OL	GRELL3D+CUGD	12KM/3KM/BOTH	YES	MM+POL+SPC with 3 outer loops

503
504
505
506
507
508
509
510
511

Table 3: Statistics referred to experiments in column 1: Forecast Accuracy (ACC), Frequency Bias (FBIAS), Equitable Threat Score (ETS), False Alarm Ratio (FAR) are considered as a function of thresholds (1mm/12h and 20mm/12h). The experiments are: CTL, CON_HR_12KM, CONMM_HR_12KM, CONMMPOL_HR_12KM, CONMMPOLSPC_HR_12KM, CONMMPOLSPC3OL_HR_12KM.

Experiment	ACC *Thresholds mm/12h*		FBIAS *Thresholds mm/12h*		ETS *Thresholds mm/12h*		FAR *Thresholds mm/12h*	
	1	*20*	*1*	*20*	*1*	*20*	*1*	*20*
CTL	0.83	0.94	0.94	1.13	0.33	0.19	0.21	0.03
CON_HR_12KM	0.81	0.93	0.91	1.12	0.25	0.17	0.26	0.04
CONMM_HR_12KM	0.82	0.94	0.95	0.99	0.28	0.17	0.24	0.03
CONMMPOL_HR_12KM	0.80	0.95	0.82	0.61	0.20	0.10	0.25	0.02
CONMMPOLSPC_HR_12KM	0.82	0.94	0.86	0.92	0.28	0.14	0.21	0.03
CONMMPOLSPC3OL_HR_12KM	0.82	0.95	0.93	0.84	0.30	0.16	0.20	0.03

Table 4: Statistics referred to experiments in column 2: Forecast Accuracy (ACC), Frequency Bias (FBIAS), Equitable Threat Score (ETS), False Alarm Ratio (FAR) are considered as a function of thresholds (1mm/12h and 20mm/12h). The experiments are: CTL, CON_3KM, CONMM_3KM, CONMMPOL_3KM, CONMMPOLSPC_3KM, CONMMPOLSPC3OL_3KM.

Experiment	ACC *Thresholds mm/12h*		FBIAS *Thresholds mm/12h*		ETS *Thresholds mm/12h*		FAR *Thresholds mm/12h*	
	1	*20*	*1*	*20*	*1*	*20*	*1*	*20*
CTL	0.83	0.94	0.94	1.13	0.33	0.19	0.21	0.03
CON_3KM	0.82	0.94	0.80	0.83	0.24	0.15	0.22	0.03
CONMM_3KM	0.82	0.94	0.96	0.96	0.26	0.17	0.24	0.03
CONMMPOL_3KM	0.81	0.95	0.94	0.84	0.23	0.11	0.24	0.03
CONMMPOLSPC_3KM	0.82	0.94	1.03	0.90	0.28	0.16	0.24	0.03
CONMMPOLSPC3OL_3KM	0.83	0.95	0.96	0.91	0.27	0.18	0.27	0.03

Table 5: Statistics referred to experiments in column 3: Forecast Accuracy (ACC), Frequency Bias (FBIAS), Equitable Threat Score (ETS), False Alarm Ratio (FAR) are considered as a function of thresholds (1mm/12h and 20mm/12h). The experiments are: CTL, CON_12KM_3KM, CONMM_12KM_3KM, CONMMPOL_12KM_3KM, CONMMPOLSPC_12KM_3KM, CONMMPOLSPC3OL_12KM_3KM.

Experiment	ACC *Thresholds mm/12h*		FBIAS *Thresholds mm/12h*		ETS *Thresholds mm/12h*		FAR *Thresholds mm/12h*	
	1	*20*	*1*	*20*	*1*	*20*	*1*	*20*
CTL	0.83	0.94	0.94	1.13	0.33	0.19	0.21	0.03

CON_12KM_3KM	0.81	0.95	0.84	0.73	0.20	0.14	0.27	0.02
CONMM_12KM_3KM	0.83	0.94	0.96	0.94	0.28	0.16	0.23	0.03
CONMMPOL_12KM_3KM	0.81	0.95	0.96	0.75	0.23	0.13	0.25	0.03
CONMMPOLSPC_12KM_3KM	0.81	0.95	1.04	0.79	0.26	0.17	0.28	0.02
CONMMPOLSPC3OL_12KM_3KM	0.83	0.95	0.98	0.73	0.30	0.18	0.25	0.02

Table 6: Statistics referred to experiments in line 1: Forecast Accuracy (ACC), Frequency Bias (FBIAS), Equitable Threat Score (ETS), False Alarm Ratio (FAR) are considered as a function of thresholds (1mm/12h and 20mm/12h). The experiments are: CTL, CON_3KM, CON_HR_12KM, CON_12KM_3KM.

Experiment	**ACC** ***Thresholds mm/12h***		**FBIAS** ***Thresholds mm/12h***		**ETS** ***Thresholds mm/12h***		**FAR** ***Thresholds mm/12h***	
	1	***20***	***1***	***20***	***1***	***20***	***1***	***20***
CTL	0.83	0.94	0.94	1.13	0.33	0.19	0.21	0.03
CON_3KM	0.82	0.94	0.80	0.83	0.24	0.15	0.22	0.03
CON_HR_12KM	0.81	0.93	0.91	1.12	0.25	0.17	0.26	0.04
CON_12KM_3KM	0.81	0.95	0.84	0.73	0.20	0.14	0.27	0.02

Table 7: Statistics referred to experiments in line 2: Forecast Accuracy (ACC), Frequency Bias (FBIAS), Equitable Threat Score (ETS), False Alarm Ratio (FAR) are considered as a function of thresholds (1mm/12h and 20mm/12h). The experiments are: CTL, CONMM_3KM, CONMM_HR_12KM, CONMM_12KM_3KM.

Experiment	**ACC** ***Thresholds mm/12h***		**FBIAS** ***Thresholds mm/12h***		**ETS** ***Thresholds mm/12h***		**FAR** ***Thresholds mm/12h***	
	1	***20***	***1***	***20***	***1***	***20***	***1***	***20***
CTL	0.83	0.94	0.94	1.13	0.33	0.19	0.21	0.03
CONMM_3KM	0.82	0.94	0.96	0.96	0.26	0.17	0.24	0.03
CONMM_HR_12KM	0.82	0.94	0.95	0.99	0.28	0.17	0.24	0.03
CONMM_12KM_3KM	0.83	0.94	0.96	0.94	0.28	0.16	0.23	0.03

Table 8: Statistics referred to experiments in line 3: Forecast Accuracy (ACC), Frequency Bias (FBIAS), Equitable Threat Score (ETS), False Alarm Ratio (FAR) are considered as a function of thresholds (1mm/12h and 20mm/12h). The experiments are: CTL, CONMMPOL_3KM, CONMMPOL_HR_12KM, CONMMPOL_12KM_3KM.

Experiment	**ACC** ***Thresholds mm/12h***		**FBIAS** ***Thresholds mm/12h***		**ETS** ***Thresholds mm/12h***		**FAR** ***Thresholds mm/12h***	
	1	***20***	***1***	***20***	***1***	***20***	***1***	***20***
CTL	0.83	0.94	0.94	1.13	0.33	0.19	0.21	0.03

CONMMPOL_3KM	0.81	0.95	0.94	0.84	0.23	0.11	0.24	0.03
CONMMPOL_HR_12KM	0.80	0.95	0.82	0.61	0.20	0.10	0.25	0.02
CONMMPOL_12KM_3KM	0.81	0.95	0.96	0.75	0.23	0.13	0.25	0.03

Table 9: Statistics referred to experiments in line4: Forecast Accuracy (ACC), Frequency Bias (FBIAS), Equitable Threat Score (ETS), False Alarm Ratio (FAR) are considered as a function of thresholds (1mm/12h and 20mm/12h). The experiments are: CTL, CONMMPOLSPC_3KM, CONMMPOLSPC_HR_12KM, CONMMPOLSPC_12KM_3KM.

Experiment	**ACC** ***Thresholds mm/12h***		**FBIAS** ***Thresholds mm/12h***		**ETS** ***Thresholds mm/12h***		**FAR** ***Thresholds mm/12h***	
	1	***20***	***1***	***20***	***1***	***20***	***1***	***20***
CTL	0.83	0.94	0.94	1.13	0.33	0.19	0.21	0.03
CONMMPOLSPC_3KM	0.82	0.94	1.03	0.90	0.28	0.16	0.25	0.03
CONMMPOLSPC_HR_12KM	0.82	0.94	0.86	0.92	0.28	0.14	0.21	0.03
CONMMPOLSPC_12KM_3KM	0.81	0.95	1.04	0.79	0.26	0.17	0.28	0.02

Table 10: Statistics referred to experiments in line 5: Forecast Accuracy (ACC), Frequency Bias (FBIAS), Equitable Threat Score (ETS), False Alarm Ratio (FAR) are considered as a function of thresholds (1mm/12h and 20mm/12h). The experiments are: CTL, CONMMPOLSPC3OL_3KM, CONMMPOLSPC3OL_HR_12KM, CONMMPOLSPC3OL_12KM_3KM.

Experiment	**ACC** ***Thresholds mm/12h***		**FBIAS** ***Thresholds mm/12h***		**ETS** ***Thresholds mm/12h***		**FAR** ***Thresholds mm/12h***	
	1	***20***	***1***	***20***	***1***	***20***	***1***	***20***
CTL	0.83	0.94	0.94	1.13	0.33	0.19	0.21	0.03
CONMMPOLSPC3OL_3KM	0.83	0.95	0.96	0.91	0.27	0.18	0.27	0.03
CONMMPOLSPC3OL_HR_12KM	0.82	0.95	0.93	0.84	0.30	0.16	0.20	0.03
CONMMPOLSPC3OL_12KM_3KM	0.83	0.95	0.98	0.73	0.30	0.18	0.25	0.02